

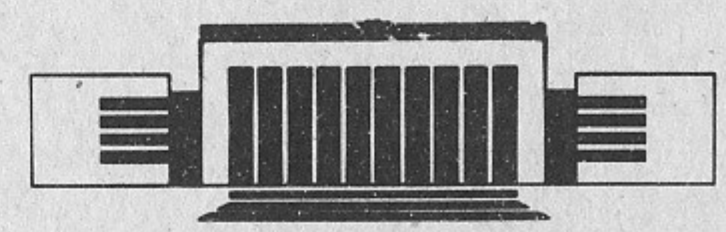
ИНСТИТУТ ЯДЕРНОЙ ФИЗИКИ
им. Г.И. Будкера СО РАН



V.F. Dmitriev

THE NUCLEAR RESPONSE AT
HIGH EXCITATION ENERGY
IN THE (^3He , t) REACTION

PREPRINT 92-22



НОВОСИБИРСК

The Nuclear Response at High Excitation Energy in the (^3He , t) Reaction

V.F. Dmitriev

Budker Institute of Nuclear Physics
630090, Novosibirsk 90, Russia

ABSTRACT

The excitation of a Δ -isobar in a finite nucleus in charge-exchange (^3He , t) reaction is discussed in terms of a nuclear response function. The medium effects modifying a Δ - and a pion propagation were considered for a finite size nucleus. The Glauber approach has been used for distortion of a ^3He and a triton in the initial and the final states. Large spreading width was found for the reaction on ^{12}C at 2 GeV of the ^3He kinetic energy.

1 INTRODUCTION

The experimental studies of nuclear response in charge-exchange reactions were extended in the eighties to high excitation energies where a first nucleon resonance the Δ -isobar can be excited [1]. The detailed studies were done for the (^3He ,t) charge-exchange reaction at different projectile energies [2] and different targets [3]. The properties of the Δ excited in a nucleus were found different compared to the case of the reaction on a single nucleon. The difference was both in the peak position and the width of the resonance excited in a complex nucleus. The review of the observed phenomena can be found in the recent review paper [4].

The appealing explanation of this phenomenon is related to medium effects, namely, the excitation of a pionic nuclear mode [5], [6], [7], [8] although another explanation has been proposed as well [9]. In this picture the Δ in nuclear matter does not exist as separate resonance but forms a collective excitation consisting of pionic, Δ and nucleon degrees of freedom.

At first sight one should not expect sizeable medium effects for (^3He ,t) reaction since the reaction takes place at the surface of the target [10]. For inelastic reactions, however, the absorption is smaller and one should use absorption factor different from that used for elastic scattering [11] providing both the medium effects and the magnitude of inelastic cross-section. Another important point is the account of the finite target size in the response function. As it will be shown below different Δ -hole multipoles are peaked at different energies so, part of the observed width can be attributed to this spreading.

Here we present the results of the absolute cross-section calculations of

the $^{12}\text{C}(^3\text{He},t)$ reaction at 0° and at the kinetic energy of the ^3He $T_{He}=2$ GeV. In the next section we discuss the model for the reaction amplitude that is a driving force for the nuclear response. In the section 4 the pionic response function of a finite nucleus is discussed and the cross-section is calculated in the section 6.

2 REACTION AMPLITUDE

We shall start from the discussion of the models for the elementary charge-exchange reaction $p(p,n)\Delta^{++}$. From the early sixties it was shown this reaction can be described by OPE model [12], at least at low momentum transfer. This analysis has been extended for wide range of the proton energies in [13], and has been repeated with some minor modifications in connection of the analysis of $p(^3\text{He},t)\Delta^{++}$ reaction in [14]. As it was shown all existing data in the region of low momentum transfer are well described by OPE with the soft monopole πNN - and $\pi N\Delta$ - form factors

$$F(q^2) = \frac{\Lambda^2 - \mu^2}{\Lambda^2 - q^2}. \quad (1)$$

The parameter $\Lambda = 650$ MeV at low proton energy and slightly decreases with the proton energy reflecting increase of the absorption effects at high energy. With these soft form factors (1) the main contribution to the Δ -production comes from the direct graph shown in Fig.1. The exchange contribution is small for the $p(p,n)\Delta^{++}$ reaction.

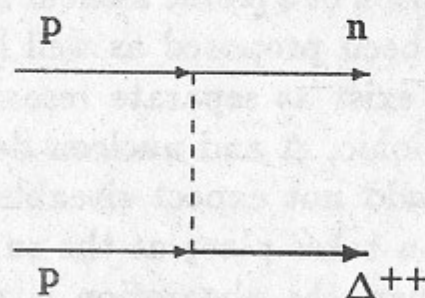


Fig. 1. Direct OPE graph for the Δ production.

In this model the amplitude is completely longitudinal with respect to the momentum transfer. In the other model used for the description of

the Δ -production at 800 MeV proton energy [15] the transverse part of the amplitude was described by ρ -exchange and hard form factors with $\Lambda = 1.2$ GeV and $\Lambda = 1.7$ GeV were used for $\pi N\Delta$ - and $\rho N\Delta$ -vertexes. The magnitude of the cross-section and the momentum transfer dependence are reproduced in this model due to cancellation between the direct and the exchange parts of the amplitude. The cancellation is rather delicate and at higher proton energy it can be broken resulting in wrong momentum transfer dependence [14].

At very high energy the situation is different. The π -exchange contribution decreases as s^{-2} , where s is the center-of-mass energy squared, while for the ρ -exchange the decrease is slower. Its contribution falls down like $s^{-2+\alpha(0)}$ for small momentum transfer where $\alpha(t)$ is the corresponding Regge-trajectory. Thus, in the asymptotic region at high energy one should expect the dominance of the ρ -exchange at forward angles. Below 20 GeV the cross-section for forward scattering follows the $1/s^2$ law [16] so, the contribution of ρ -exchange at intermediate energies is believed to be small.

For the $p(^3\text{He},t)\Delta^{++}$ reaction the situation is similar to the (p,n) case. The π -exchange with the soft form factors (1) gives reasonable description of the absolute cross-section and the tritium spectrum at forward angle for all existing data [14]. Nevertheless, at the kinetic energy of ^3He 2 GeV, which is close in kinematics to 800 MeV (p,n) one can get good description using $\pi + \rho$ exchanges as well [17]. It would be very desirable to extend the last analysis to higher ^3He energies.

3 NUCLEAR MATTER RESPONSE TO THE PIONIC PROBE

3.1 $(^3\text{He}, t)$ Cross-Section in Plane Wave Approximation

It is convenient to start with the plane waves for both projectile and ejectile in order to obtain an expression for the cross-section that can be easily generalized to the distorted waves. In PWIA the cross-section is proportional to the matrix element, shown in Fig.1, squared and summed over final nuclear and Δ -states.

$$T = \int d^3r \Gamma_{\pi H\alpha}(r) \cdot G_0(r - r') \cdot \Gamma_{\pi N\Delta}(r') d^3r'. \quad (2)$$

For plane waves $\Gamma \sim e^{i\mathbf{q}\mathbf{r}}$, it gives for the cross-section

$$\frac{d^2\sigma}{dE'd\Omega} = \frac{M_{He}^2 p'}{4\pi^2 p} |\Gamma_{\pi H\alpha}(\mathbf{q})|^2 \sum_{\Delta h} \delta(\omega - E_{\Delta h}) n_h |\Gamma_{\pi N\Delta}(\mathbf{q})|^2 \cdot |G_0(q)|^2. \quad (3)$$

The expression under the sum is just imaginary part of the pionic self-energy in nuclear medium.

$$\Im m \Pi_{\Delta}(\omega, \mathbf{q}, \mathbf{q}) = \pi \sum_{\Delta h} \delta(\omega - E_{\Delta h}) |\Gamma_{\pi N\Delta}|^2 n_h. \quad (4)$$

Using the pionic self-energy (4) we obtain the final expression for the cross-section suitable for inclusion of medium effects.

$$\frac{d^2\sigma}{dE'd\Omega} = \frac{M_{He}^2 p'}{4\pi^3 p} |\Gamma_{\pi H\alpha}(\mathbf{q})|^2 G_0^*(q) \cdot \Im m \Pi_{\Delta}(\omega, \mathbf{q}, \mathbf{q}) \cdot G_0(q). \quad (5)$$

3.2 Medium Effects in Nuclear Matter

The main effect of nuclear medium is the renormalization of the pion propagator by intermediate Δ -hole loops giving the major contribution to the pionic self-energy (4) near the Δ -resonance. To take it into account one must change in (5) the bare pion propagator $G_0(q)$ for the dressed one $G(\omega, \mathbf{q})$, where

$$G(\omega, \mathbf{q}) = \frac{1}{q^2 - \mu^2 - \Pi_{\Delta}(\omega, \mathbf{q})}.$$

Making this change we are going out of the scope of the impulse approximation.

The imaginary part of the bare pion propagator is equal to zero for negative q^2 . Using it we obtain $G^*(\omega, \mathbf{q}) \cdot \Im m \Pi_{\Delta}(\omega, \mathbf{q}) \cdot G(\omega, \mathbf{q}) = -\Im m G(\omega, \mathbf{q})$. With these changes the cross-section (5) becomes

$$\frac{d^2\sigma}{dE'd\Omega} = -\frac{M_{He}^2 p'}{4\pi^3 p} |\Gamma_{\pi H\alpha}(\mathbf{q})|^2 \cdot \Im m G(\omega, \mathbf{q}). \quad (6)$$

It is clear from (6) the pion propagator $G(\omega, \mathbf{q})$ in nuclear medium is just the response function to a virtual pion probe. The excitation created by a virtual pion is no more pure Δ -hole but a superposition of the Δ -hole and pionic degrees of freedom, which is usually called the pionic mode.

The unquenched Δ -hole self-energy (4) produces too much of attraction giving unreasonably low excitation energy for the pionic mode. In order to make the description more accurate several effects should be taken into

account. First of all, more correct πN -scattering amplitude reproducing $s_{\frac{1}{2}}$ and $p_{\frac{1}{2}}$ partial waves should be used since we are interested in the energies lower than the Δ in vacuum. For this purpose one should add the Born diagrams with a nucleon intermediate state, u -channel Δ diagram and a σ -term arising from the σ -commutator [18]. Second, the short-range $N\Delta$ -correlations must be taken into account.

$$W(\mathbf{r}_1, \mathbf{r}_2) = \frac{f_{\Delta}^2}{\mu^2} g'_{\Delta} (\mathbf{S}_1^{\dagger} \cdot \mathbf{S}_2) (\mathbf{T}_1^{\dagger} \cdot \mathbf{T}_2) \delta(\mathbf{r}_1 - \mathbf{r}_2). \quad (7)$$

In nuclear matter the effect of short-range correlations can be accounted in the following way. Let us define the Δ -hole response function by

$$\Pi_{\Delta}(\omega, \mathbf{q}) = \left(\frac{\Lambda^2 - \mu^2}{\Lambda^2 - q^2} \right)^2 q^2 \cdot \chi(\omega, \mathbf{q}).$$

Then,

$$\tilde{\Pi}_{\Delta}(\omega, \mathbf{q}) = \frac{\Pi_{\Delta}(\omega, \mathbf{q})}{1 - g' \cdot \chi(\omega, \mathbf{q})}. \quad (8)$$

Similar effect should be taken into account for the nucleon-hole response function as well. But, in the region of interest in excitation energy its contribution is negligible and will be omitted below. In contrast, the backward Δ -hole loops and the σ -term must be retained since they have their own dependence on the virtual pion mass $-q^2$ that influences the position of the pionic branch in nuclear matter.

Finally, the virtual pion can be absorbed in nuclear medium via two-nucleon mechanism without the Δ -production. To take it into account we use the Ericson-Ericson optical potential from pionic atoms [19]

$$V_{2N} = -4\pi i \text{Im} C \cdot n^2(r) \cdot q^2,$$

where $\text{Im} C = 0.08 \cdot \left(\frac{\hbar}{\mu c} \right)^6$, and $n(r)$ is the nuclear matter density. With these corrections the pion self-energy in nuclear matter is

$$\Pi(\omega, \mathbf{q}) = \tilde{\Pi}_{\Delta}(\omega, \mathbf{q}) + \frac{1}{f_{\pi}^2} \left(1 - \frac{2q^2}{\mu^2} \right) \sigma(0) \cdot n(r) + V_{2N}, \quad (9)$$

where f_{π} is the pion decay constant $f_{\pi} = 133$ MeV and $\sigma(0)$ is the σ -commutator for forward pion scattering, $\sigma(0) = 66$ MeV. $\tilde{\Pi}_{\Delta}(\omega, \mathbf{q})$ includes both forward and backward Δ -hole loops corrected for short-range correlations.

4 RESPONSE FUNCTION OF A FINITE NUCLEUS

For a finite nucleus it is convenient to work in the configuration space where the self-energy (9) and the pion propagator become the functions of two distinct variables instead of functions of the distance between coordinate points in nuclear matter.

$$\Pi(\omega, \mathbf{r} - \mathbf{r}') \rightarrow \Pi(\omega, \mathbf{r}, \mathbf{r}');$$

$$V_{2N} = 4\pi i m C (\nabla \cdot \mathbf{n}^2(\mathbf{r}) \cdot \nabla) \delta(\mathbf{r} - \mathbf{r}').$$

The $\pi N \Delta$ - vertex in the configuration space is

$$\Gamma_{\pi N \Delta}(\mathbf{r}, \mathbf{r}') = -i \mathbf{T}(\mathbf{S} \cdot \nabla) \frac{f_{\Delta}}{\mu} \frac{\Lambda^2 - \mu^2}{4\pi} \frac{\exp(-\kappa |\mathbf{r} - \mathbf{r}'|)}{|\mathbf{r} - \mathbf{r}'|}, \quad (10)$$

where $\kappa^2 = \Lambda^2 - \omega^2$.

4.1 Multipole Expansion

For a spherical nucleus the self-energy (9) has simple multipole expansion

$$\Pi(\omega, \mathbf{r}, \mathbf{r}') = \sum_{JM} \Pi_J(\mathbf{r}, \mathbf{r}') Y_{JM}^*(\mathbf{n}) Y_{JM}(\mathbf{n}').$$

The similar expansion exists for the $\pi N \Delta$ -vertex

$$\Gamma_{\pi N \Delta}(\mathbf{r} - \mathbf{r}') = \sum_{JLM} \Gamma_{JL}^0(\mathbf{r}, \mathbf{r}') Y_{JM}^*(\mathbf{n}) T_{JM}^L(\mathbf{n}'), \quad (11)$$

where the tensor operator

$$T_{JM}^L(\mathbf{n}') = \mathbf{S} \cdot \mathbf{Y}_{JM}^L(\mathbf{n}) = [\mathbf{S} \wedge \mathbf{Y}_{Lm}(\mathbf{n})]_{JM}, \quad (12)$$

and the radial vertex $\Gamma_{JL}^0(\mathbf{r}, \mathbf{r}')$ is

$$\begin{aligned} \Gamma_{JL}^0(\mathbf{r}, \mathbf{r}') &= \\ &= i(L-J) \frac{f_{\Delta}}{\mu} \frac{2\kappa^2(\Lambda^2 - \mu^2)}{\pi} \sqrt{\frac{J+L+1}{2(2J+1)}} \begin{cases} i_L(\kappa r) k_J(\kappa r') & \text{if } r < r', \\ -i_J(\kappa r') k_L(\kappa r) & \text{if } r > r', \end{cases} \end{aligned} \quad (13)$$

here $i_L(x)$ and $k_L(x)$ are the spherical Bessel functions with an imaginary argument.

The Δ -hole response function χ can be expanded using the set of tensor operators (12)

$$\begin{aligned} \chi_{LL'}^J(\mathbf{r}, \mathbf{r}') &= \\ &= \frac{1}{2J+1} \sum_{j_N l_N l_{\Delta}} \langle j_N l_N || T_J^L || j_{\Delta} l_{\Delta} \rangle \langle j_{\Delta} l_{\Delta} || T_J^{L'} || j_N l_N \rangle [g_{j_{\Delta} l_{\Delta}}(\omega + \epsilon_{j_N l_N}; \mathbf{r}, \mathbf{r}') + \\ &\quad + g_{j_{\Delta} l_{\Delta}}(-\omega + \epsilon_{j_N l_N}; \mathbf{r}, \mathbf{r}')] \cdot n_{j_N l_N} \cdot R_{j_N l_N}(\mathbf{r}) R_{j_N l_N}(\mathbf{r}'), \end{aligned} \quad (14)$$

where $n_{j_N l_N}$ are the nucleon occupation numbers, $R_{j_N l_N}(\mathbf{r})$ the radial wave function of bounded nucleon and the $\epsilon_{j_N l_N}$ is its energy. $g_{j_{\Delta} l_{\Delta}}(\omega; \mathbf{r}, \mathbf{r}')$ is the Green function of the radial Schrödinger equation for the Δ moving in the mean nuclear potential. It was calculated using two independent solutions of the radial Schrödinger equation.

The Δ -hole contribution to the pion self-energy can be calculated using the following expression

$$\bar{\Pi}_{\Delta}^J(\omega; \mathbf{r}, \mathbf{r}') = \sum_{LL'} \int \rho^2 d\rho \rho'^2 d\rho' \Gamma_{JL}^0(\mathbf{r}, \rho) \chi_{LL'}^J(\rho, \rho') \Gamma_{JL'}^*(\rho, \mathbf{r}'); \quad (15)$$

where Γ_{JL} related to Γ_{JL}^0 via linear integral equation accounting the short-range correlations (7)

$$\Gamma_{JL}(\mathbf{r}, \rho) = \Gamma_{JL}^0(\mathbf{r}, \rho) + g' \left(\frac{f_{\Delta}}{\mu} \right)^2 \sum_{L'} \int \rho'^2 d\rho' \Gamma_{JL'}(\mathbf{r}, \rho') \chi_{L'L}^J(\rho', \rho). \quad (16)$$

5 THE EFFECTS OF DISTORTION

For numerical calculations it is convenient to come back from expression (6) to more complex one similar to (5)

$$\frac{d^2\sigma}{dE' d\Omega} = \frac{M_{He}^2 p'}{4\pi^2 p} \overline{\Gamma_{\pi He}^{\dagger} \cdot G^* \cdot \Im m \Pi \cdot G \cdot \Gamma_{\pi He}}. \quad (17)$$

The product sign means integration over all coordinates in the configuration space and the overline is the averaging and summing over spins of a ${}^3\text{He}$ and a triton.

In the plane wave approximation the $\pi {}^3\text{He} t$ vertex is

$$\Gamma_{\pi He}(\mathbf{r}) = \sqrt{2}(\boldsymbol{\sigma} \cdot \tilde{\mathbf{q}}) F(q^2) \frac{f_N(q^2)}{\mu} \exp(i\mathbf{q}\mathbf{r}), \quad (18)$$

where the effective momentum transfer \tilde{q} in lab. system is

$$\tilde{q} = \sqrt{\frac{E' + M}{E + M}} p - \sqrt{\frac{E + M}{E' + M}} p',$$

here E is the total energy of ${}^3\text{He}$ and M is its mass. At first order in $\frac{\omega}{E+M}$ it can be rewritten as

$$\tilde{q} = q - \frac{1}{2} \frac{\omega}{E + M} (p + p')$$

The effective momentum transfer squared coincides with the four-momentum transfer squared. $F(q^2)$ is the $({}^3\text{He}, t)$ transition form factor.

The multipole expansion of the vertex looks as follows

$$\Gamma_{\pi H\alpha}(\mathbf{r}) = \sum_{JLM} \Gamma_{LJM}^N(\mathbf{r}) t_{JM}^L(\mathbf{n}), \quad (19)$$

where $t_{JM}^L(\mathbf{n})$ are the tensor operators analogous to the (12)

$$t_{JM}^L(\mathbf{n}) = (\boldsymbol{\sigma} \cdot \mathbf{Y}_{JM}^L(\mathbf{n})) = [\boldsymbol{\sigma} \wedge Y_{LM}]_{JM}. \quad (20)$$

For plane waves the radial vertex is

$$\Gamma_{JLM}^{0N}(\mathbf{r}) = \sqrt{2} (i)^L j_L(qr) [\tilde{q} \wedge Y_{LM}^*(\hat{q})]_{JM} \frac{f_N(q^2)}{\mu} F(q^2) \quad (21)$$

The distortion of the incoming and outgoing waves has been taken into account via inelastic distortion factor [11]. With this factor the $\pi{}^3\text{He}t$ vertex is

$$\begin{aligned} \Gamma_{\pi H\alpha}(\mathbf{r}) &= \\ &= \sqrt{2} \left[-i(\boldsymbol{\sigma} \cdot \nabla) - \frac{1}{2} \frac{\omega}{E + M} (\boldsymbol{\sigma} \cdot (p + p')) \right] \frac{f_N(q^2)}{\mu} \exp(iqr) \exp\left(-\frac{1}{2} \chi_{in}(\mathbf{r}_\perp, q)\right). \end{aligned} \quad (22)$$

The distortion factor $\exp(-\frac{1}{2} \chi_{in}(\mathbf{r}_\perp, q))$ has been found in [11]

$$\begin{aligned} \exp\left(-\frac{1}{2} \chi_{in}(\mathbf{r}_\perp, q)\right) &= \\ &= \left(1 - \frac{1}{A} \bar{\gamma} T(\mathbf{r}_\perp)\right)^{A-1} \int d^3 s_1 d^3 s_2 d^3 s_3 \exp(iq s_1) \Psi^*(s_1, s_2, s_3) \times \end{aligned}$$

$$\begin{aligned} &\times \left(1 - \frac{1}{A} \bar{\gamma} T(\mathbf{r}_\perp + s_{2\perp} - s_{1\perp})\right)^A \cdot \left(1 - \frac{1}{A} \bar{\gamma} T(\mathbf{r}_\perp + s_{3\perp} - s_{1\perp})\right)^A \times \\ &\times \Psi(s_1, s_2, s_3) \delta(s_1 + s_2 + s_3), \end{aligned} \quad (23)$$

where $T(\mathbf{r}_\perp)$ is the thickness function

$$T(\mathbf{r}_\perp) = \int_{-\infty}^{\infty} \rho(\mathbf{r}_\perp, z) dz,$$

and $\rho(\mathbf{r}_\perp, z)$ is the target density. The

$$\bar{\gamma} = -i \frac{2\pi}{p_{lab}} f(0)$$

is related to the elastic nucleon-nucleon scattering amplitude at given energy per nucleon and $\Psi(s_1, s_2, s_3)$ is the wave function of the ${}^3\text{He}$ or the triton depending on the internal coordinates s . The value of $\bar{\gamma}$ used in calculations is $\bar{\gamma} = (2.1 - i0.26) fm^2$ [21].

Two features of the distortion factor (23) should be mentioned. First, the ${}^3\text{He}t$ form factor can not be separated from the effects of distortion. Second, since the vertex (22) has a gradient coupling and the distortion factor (23) depends on the transversal coordinates, some transversal components arise in the reaction amplitude even if it was before pure longitudinal amplitude.

The multipole expansion of the distorted vertex (22) can be obtained directly by multiplying it on $t_{JM}^L(\mathbf{n})$, taking trace over spin matrices, and integrating over angles of the unit radius vector \mathbf{n} .

$$\Gamma_{LJM}^N(\mathbf{r}) = \frac{1}{2} \text{Tr} \int d\mathbf{n} \left(t_{JM}^L(\mathbf{n}) \cdot \Gamma_{\pi H\alpha}(\mathbf{r}) \right). \quad (24)$$

The separate multipoles contribute independently into cross-section (17), which becomes

$$\frac{d^2\sigma}{dE' d\Omega} = \frac{M_{He}^2 p'}{4\pi^3 p} \sum_{LJM} \Gamma_{LJM}^{*N} \cdot G_L^* \cdot \mathfrak{S} m \Pi_L \cdot G_L \cdot \Gamma_{LJM}^N. \quad (25)$$

For numerical calculation it is convenient to define the function

$$w_{LJM}(\mathbf{r}) = \int_0^\infty r'^2 dr' G_L(\mathbf{r}, r') \Gamma_{LJM}^N(r'),$$

which is the pion field at the reaction point generated by the source $\Gamma_{LJM}^N(r')$. The function $w_{LJM}(r)$ satisfies the integro-differential equation

$$\int_0^\infty r'^2 dr' G_L^{-1}(r, r') w_{LJM}(r') = \Gamma_{LJM}^N(r), \quad (26)$$

which was solved numerically using the condition for Feynman propagator $G_L(r, r') = G_L^{(+)}(r, r')$ at positive energy. Since $G_L^{(+)}(r, r')$ has an outgoing wave at infinity it fixes the solution of the equation (26). The cross-section expressed in terms of $w_{LJM}(r)$ is

$$\frac{d^2\sigma}{dE'd\Omega} = \frac{M_{He}^2}{4\pi^3} \frac{p'}{p} \sum_{LJM} w_{LJM}^* \cdot \Im m \Pi_L \cdot w_{LJM}. \quad (27)$$

In the expression (27) the integration over coordinates goes effectively in a finite range, inside the target nucleus.

6 THE TRITON SPECTRA FOR $^{12}\text{C}(^3\text{He}, t)$ REACTION AT 2 GeV

6.1 Parameters of the single-particle potentials.

The nucleon single-particle potential used for the wave functions of the bound nucleons has been taken in the standard Woods-Saxon form.

$$U(r) = V_0 \cdot f(r) + V_{LS} \frac{\lambda_\pi^2}{r} \frac{df(r)}{dr} (\sigma \cdot l) + V_C(r),$$

where $f(r) = \frac{1}{1 + \exp(r-R/a)}$, λ_π is the pion Compton wavelength, and $V_C(r)$ is the Coulomb potential for protons that was taken as the potential of a uniformly charged sphere. The parameters of the potential are listed in the Table 1. The response function (14) were found not very sensitive to the parameters of the nucleon potential.

The optical Δ -nucleus potential has been taken in similar Woods-Saxon form.

$$U_\Delta(r) = (V_\Delta + iW_\Delta) \cdot f(r) + (V_{\Delta LS} + iW_{\Delta LS}) \frac{\lambda_\pi^2}{r} \frac{df(r)}{dr} (s_\Delta \cdot l) + V_{\Delta C}(r),$$

where s_Δ are the spin 3/2 matrices. The parameters of the optical potential

are listed in Table 2. They were taken mainly from [7], and [20] with some important changes. For the first calculations the spin-orbit potential has

Table 1. Parameters of the Single-Particle Nucleon Potential

	V_0 (MeV)	V_{LS} (MeV)	R (fm)	R_{LS} (fm)	a (fm)	a_{LS} (fm)
p	50	7	$1.25 \cdot A^{1/3}$	$1.25 \cdot A^{1/3}$	0.53	0.53
n	50	7	$1.25 \cdot A^{1/3}$	$1.25 \cdot A^{1/3}$	0.53	0.53

Table 2. Parameters of the Δ -Nucleus Optical Potential.

(The radius and diffuseness are the same as for the nucleons)

V_Δ (MeV)	W_Δ (MeV)	$V_{LS\Delta}$ (MeV)	$W_{LS\Delta}$ (MeV)
25	0	0	0

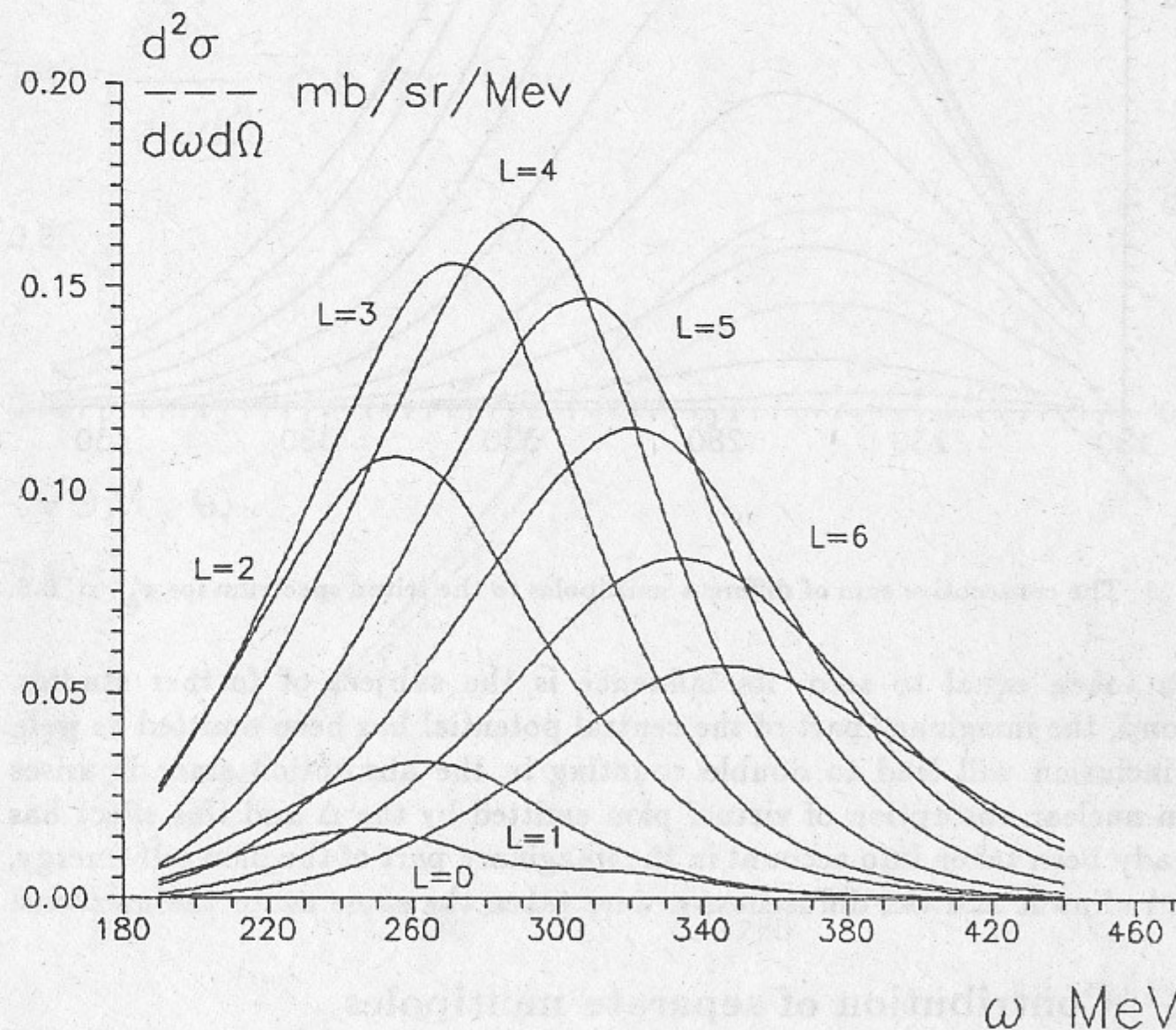


Fig. 2. The contribution of separate multiplicities to the triton spectrum. The curves correspond to the short-range correlation parameter $g'_\Delta = 0.6$.

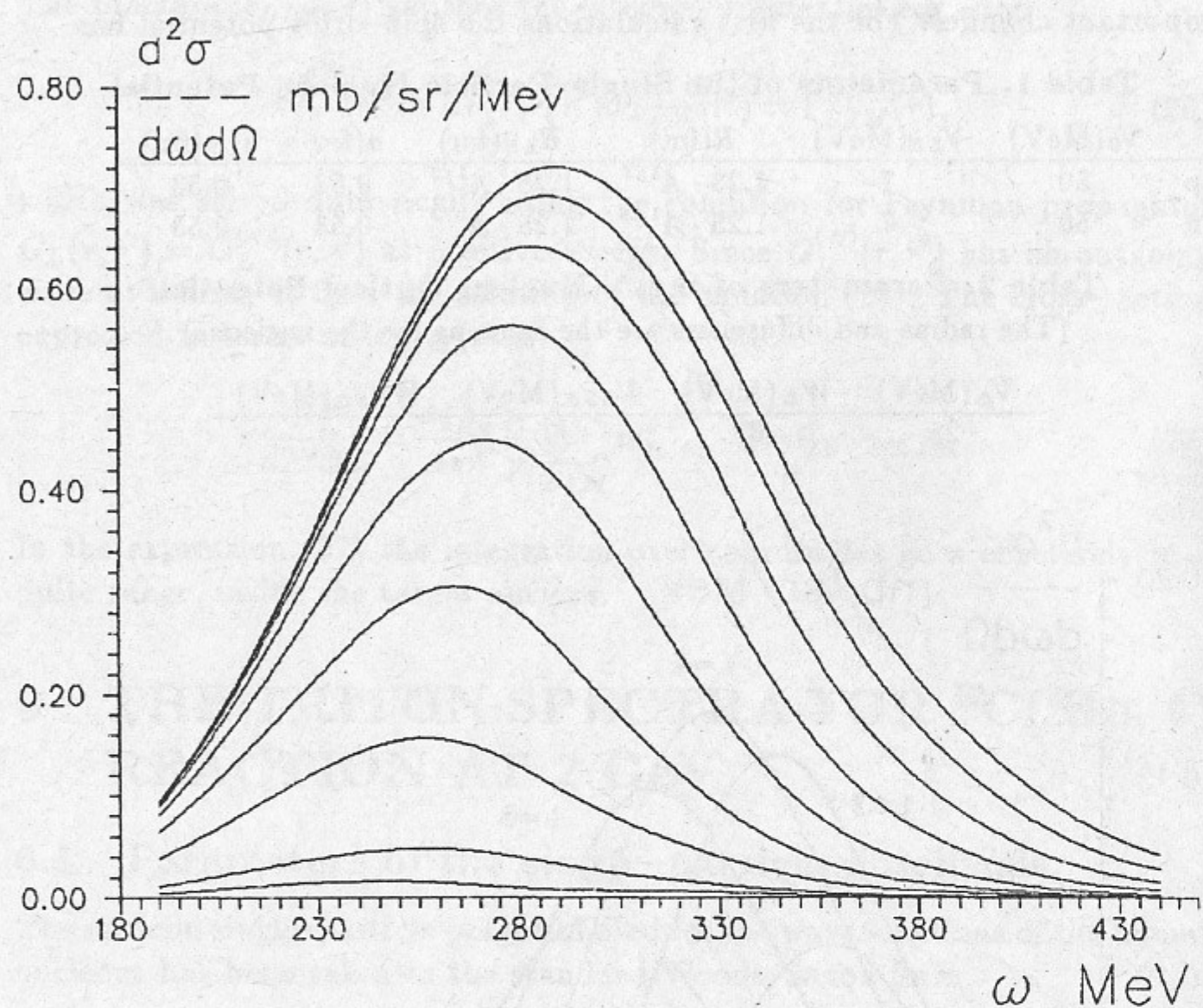


Fig. 3. The consecutive sum of different multipoles to the triton spectrum for $g'_{\Delta} = 0.6$.

been taken equal to zero, its influence is the subject of further studies. Second, the imaginary part of the central potential has been omitted as well. Its inclusion will lead to double counting in the absorption since it arises from nuclear absorption of virtual pion emitted by the Δ and this effect has already been taken into account in the imaginary part of the pion self-energy. The radius R and the diffuseness a were taken the same as for the nucleons.

6.2 Contribution of separate multipoles

The contribution of separate multipoles to the triton spectrum is shown in the Fig. 2. The contribution of the low multipoles $L = 0$ and $L = 1$ is almost negligible due to strong absorption of the incoming and the outgoing

nuclei. The main contribution comes from the multipoles from $L = 2$ to $L = 6$ although higher multipoles, at least up to $L = 8$, have to be considered.

Another feature clearly seen in the Fig. 2 is rather wide spreading of the different multipole contributions. The $L = 2$ contribution appears to be most sensitive to the medium effects shifting down the transition strength. It has the largest downward shift in the peak position. The absorption of the ${}^3\text{He}$ and t is smaller for $L = 2$ resulting in sizeable contribution to the cross-section. Higher multipoles have smaller medium effects and their peak positions are at more and more high excitation energies. This produce large spreading width of summed triton spectrum. The sum of consecutive multipole contributions up to $L = 8$ is shown in Fig. 3. Every next multipole shifts the high energy wing of the peak increasing its width.

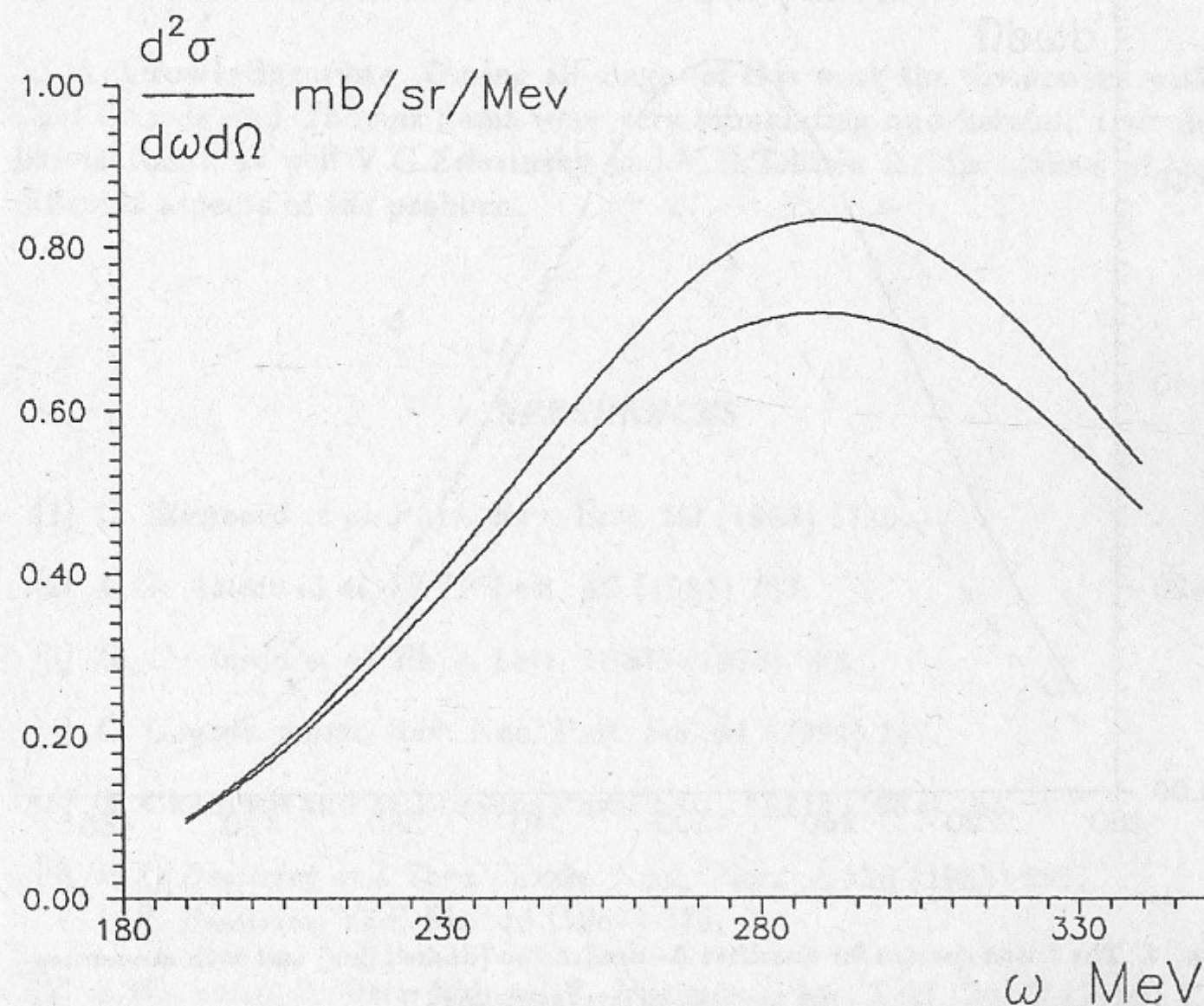


Fig. 4. The triton spectra for two values of the g'_{Δ} . Upper curve corresponds to $g'_{\Delta} = 0$, for lower curve $g'_{\Delta} = 0.6$.

The curves shown in Fig.2 and Fig.3 were obtained for the short-range correlation constant $g'_{\Delta} = 0.6$. The influence of the short-range correlations is demonstrated in Fig.4 where the summed triton spectrum for $g'_{\Delta} = 0$ and $g'_{\Delta} = 0.6$ is shown. It does not influence much the peak position but changes its height.

The influence of the medium effects leading to renormalization of the pion propagator is shown on Fig.5. The considerable shift of the peak position is visible clearly producing in addition larger cross-section compared to the quasifree case.

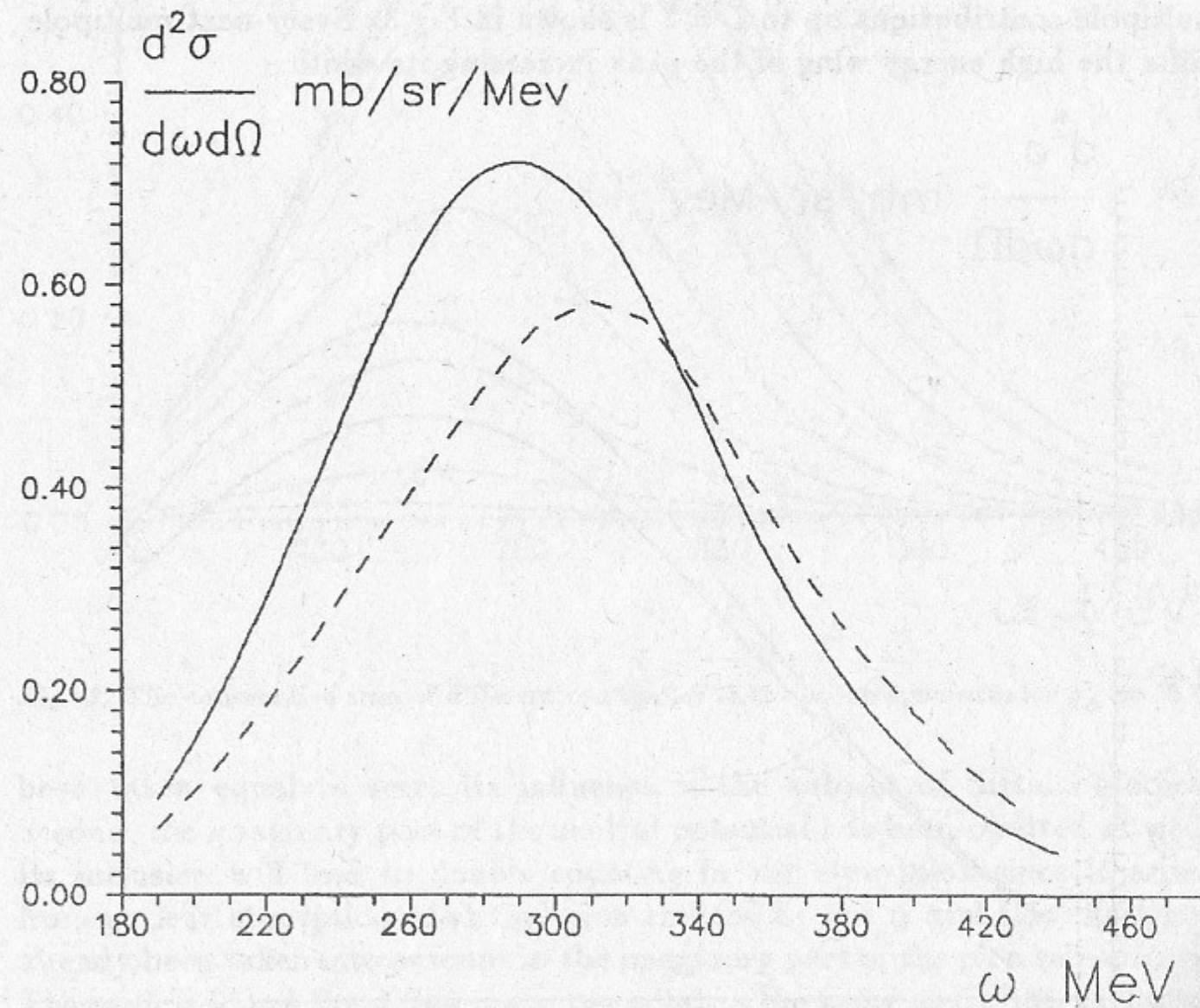


Fig. 5. The triton spectra for quasifree Δ - production (dashed line) and with accounting the medium effects (solid line).

7 CONCLUSIONS

For (${}^3\text{He}, t$) reaction in the Δ -region strong deviations from impulse approximations were demonstrated. The deviations come from the medium effects of renormalization of the pion propagator in the OPE mechanism of the elementary charge-exchange reaction. The medium effects change both the peak position and its height.

The finite size of a target nucleus produces together with the medium effects large spreading of the observed peak. The absorption in initial and final states strongly suppresses the lowest multiplicities of the angular momentum transfer. The Glauber approach to the distortion in initial and final states gives correct description both the size of the medium effects and the absolute value of the cross-section.

Acknowledgments. During all stages of this work the discussions with Carl Gaarde and Thomas Sams were very stimulating and helpful. I would like to thank as well V.G.Zelevinsky and V.B.Telitsin for discussions of the different aspects of the problem.

REFERENCES

- [1] C. Ellegaard et al. Phys. Rev. Lett. 50 (1983) 1745.
- [2] V.G. Ableev et al. JETP Lett. 40 (1984) 763.
- [3] D. Contardo et al. Phys. Lett. 168B (1986) 331.
- [4] C. Gaarde. Annu. Rev. Nuc. Part. Sci.,41 (1991) 187.
- [5] G. Chanfray and M.Ericson, Phys. Lett. 141B (1984) 163.
- [6] V.F. Dmitriev and Toru Suzuki. Nucl. Phys. A438 (1985) 697.
V.F. Dmitriev. Yad. Fiz. 46 (1987) 770.
- [7] S.W. Hong, F. Osterfeld and T. Udagawa. Phys. Lett. 245B (1990) 1.
- [8] J. Delorm and P.A.M. Guichon. Phys. Lett. 263B (1991) 157.
- [9] E. Oset, E. Shiino and H. Toki Phys. Lett. 224B (1989) 249.

- [10] *H. Esbensen and T.-S.H. Lee.* Phys. Rev. C32 (1985) 1966.
- [11] *V.F. Dmitriev.* Phys. Lett. 226B (1989) 219.
- [12] *E. Ferrari, F. Selleri.* Phys. Rev. Lett. 7 (1961) 387.
- [13] *G. Wolf* Phys. Rev. 182 (1969) 1538.
- [14] *V.F. Dmitriev, O.P. Sushkov and C. Gaarde.* Nucl. Phys. A459 (1986) 503.
- [15] *B.J. Vervest.* Phys. Lett. 83B (1979) 161.
- [16] *V.A. Karmanov et al.* Sov. Journ. Nucl. Phys. 18 (1973) 1133.
- [17] *P. Desgrolard, J. Delorme and C. Gignoux.* Preprint Inst. de Phys. Nucl. de Lyon, LYCEN 9205 (1992).
- [18] *M.G. Olsson, E.T. Osypowsky.* Nucl. Phys. B101 (1975) 136.
- [19] *M. Ericson and T.E.O. Ericson.* Ann. Phys. 36 (1966) 323.
- [20] *J. H. Koch, E. J. Moniz and N. Ohtsuka.* Ann. of Phys. 154 (1984) 99.
- [21] *Stephen J. Wallace.* In Advances in Nuclear Physics, Plenum Press, New York, Vol. 12, 1981.

V.F. Dmitriev

**The Nuclear Response at High Excitation Energy
in the (^3He , t) Reaction**

В.Ф. Дмитриев

**Отклик ядра при высоких энергиях возбуждения
в реакции (^3He , t)**

Ответственный за выпуск С.Г. Попов

Работа поступила 9 апреля 1992 г.

Подписано в печать 10.04.1992 г.

Формат бумаги 60×90 1/16 Объем 1,5 печ.л., 1,2 уч.-изд.л.

Тираж 200 экз. Бесплатно. Заказ N 22

Обработано на IBM PC и отпечатано на
ротапинтере ИЯФ им. Г.И. Будкера СО РАН,
Новосибирск, 630090, пр. академика Лаврентьева, 11.